Journal of Geodesy (2003) 76: 569–585
DOI 10.1007/s00190-002-0279-0

Journal of Geodesy

© Springer-Verlag 2003

Satellite orbit determination using triple-differenced GPS carrier phase in pure kinematic mode

S. H. Byun

Jet Propulsion Laboratory, California Institute of Technology, MS 238-600, 4800 Oak Grove Dr, Pasadena, CA 91109, USA
e-mail: shb@cobra.jpl.nasa.gov; Tel.: 818-393-5452; Fax: 818-393-4965

Received: 13 July 2001 / Accepted: 3 June 2002

Abstract. A new algorithm and computer program, KODAC (Kinematic Orbit Determination And Comparison), was developed for precise satellite orbit determination using a kinematic approach with the ionospheric-free triple-differenced (TD) global positioning system (GPS) carrier phase as the main observable. Epoch-by-epoch satellite positions are estimated by assuming that the GPS satellite ephemerides, ground station positions, and the time series of wet tropospheric zenith delay are known in advance. The technique was demonstrated with TOPEX/POSEIDON GPS data, which gave a final radial root-mean-square orbit accuracy of 8 cm with respect to a fully dynamic solution. This new approach has the advantage of having consistent orbit accuracy regardless of satellite altitude due to its non-dynamic approach.

Keywords: Kinematic – Orbit determination – Triple difference – Global positioning system

1 Introduction

The mainstream approach to precise satellite orbit determination has been a dynamic one. In this approach, observations at different times are related to the epoch state parameters by integrating the satellite equations of motion, a process requiring accurate satellite force models. Thus, errors in the force models can introduce errors in the epoch state solution. Since the effect of force model errors tends to increase with increasing arc length, the expected error from dynamic mismodeling increases as an observation is further in time from the solution epoch. This method estimates satellite position and velocity at a single epoch from an extended arc of data, and a least-squares (LS) estimation procedure is used to find the epoch state for which the resulting model trajectory best fits the tracking data. This classic dynamic orbit determination approach has been successful for many satellite missions (Tapley 1973).

The dynamic orbit determination approach using a global positioning system (GPS) requires precise measurement models and force models for both a low Earth satellite and the GPS satellites. Precise orbit determination for TOPEX/POSEIDON using the dynamic approach with GPS was performed at the Center for Space Research (CSR), at the University of Texas at Austin. By using batch filtering software known as MSODP (Multi-Satellite Orbit Determination Program), an orbit accuracy level of 4 cm root mean square (RMS) in the radial direction was achieved. This major improvement in the satellite orbit accuracy was obtained largely by fine tuning the Earth's gravitational field and placing TOPEX/POSEIDON at a relatively high altitude of 1336 km in order to reduce the satellite dynamic model errors (Rim 1992).

The dynamic approach can provide not only the satellite orbit but also many geophysically meaningful parameters. However, precise modeling of forces acting on each satellite is a very complicated process. This approach also involves numerical integration of satellite equations of motion, and thus can be computationally extensive. When the satellite is in an environment where the precise dynamics model is not available, it is very difficult to achieve an accurate satellite orbit when a dynamic approach is used. For example, at the lower altitudes where atmospheric drag and Earth gravity anomaly effects are severe, the current dynamic model alone cannot provide an accurate satellite orbit. Even if it is possible to develop high-precision dynamic models for this environment, developing precise dynamic models, especially non-conservative force models, is an expensive and demanding task.

To improve the fit, various model parameters can be adjusted. However, the resulting solution is still a model trajectory, and its accuracy depends on how well the force models, fixed or adjusted, describe the real forces acting on the satellite. With the GPS tracking system, the use of an LS adjustment of empirical (e.g.

once-/twice-per-revolution) force parameters can compensate for the force model error, and thus can significantly reduce the orbit errors. However, more frequent relaxation tends to increase orbit error significantly, and, eventually, a purely kinematic solution would be essentially singular (Melbourne et al. 1994).

The reduced dynamic orbit determination approach has been developed by NASA's Jet Propulsion Laboratory (JPL). This approach starts with a dynamic satellite orbit determination, and then a kinematic component is introduced by adding process noise to the filter to account for errors in the force and measurement models. Thus, the reduced dynamic approach combines the satellite dynamics and the measurement geometric information, and weighs their relative strength by solving for process noise accelerations in the user satellite force model to absorb any dynamic model error. This method can produce different solution characteristics, ranging from fully dynamic to fully kinematic, by varying the parameter defining the process noise. In general, by carefully fine tuning those parameters, the solution can be optimized for a particular dynamic model accuracy. Precise orbit determination for TOPEX/POSEIDON using the reduced dynamic approach with GPS was performed at JPL with high-precision software known as GIPSY-OASIS II, and an accuracy level of 3 cm RMS in the radial direction was achieved (Bertiger et al. 1994). This reduced dynamic approach is a better choice when the dynamic model is not very accurate. However, it is computationally far more expensive than the dynamic approach, and a good dynamic model is still needed to produce a satisfactory initial reference orbit.

Since GPS signals provide comprehensive three-dimensional (3-D) geometric information, a completely new satellite orbit determination method using a kinematic approach was developed and implemented in a computer program known as KODAC (Kinematic Orbit Determination And Comparison). The algorithm does not involve any satellite force models at all, and epoch-by-epoch satellite positions are computed in purely kinematic mode by processing ionospheric-free triple-differenced (TD) GPS carrier-phase measurements as the main observables. This method requires knowledge of the GPS satellite ephemerides, ground station positions, and the time series of the wet component of the tropospheric zenith delay in advance. As with most of the other precise satellite orbit determination methods, a post-processing mode is assumed. The procedure for the kinematic satellite orbit determination approach using differenced GPS carrier phase data is composed of four main steps:

1. GPS data pre-processing
2. A priori position computing
3. Sequential batch filtering
4. Multi-epoch batch filtering

This new kinematic approach has the advantage of having consistent orbit accuracy regardless of satellite altitude, and the same algorithm can be applied to any satellite with a GPS receiver due to its non-dynamic approach. Thus, this new method is especially useful for low Earth orbiters such as the TOPEX/POSEIDON, CHAMP, ICESat (Rim et al. 2000), GRACE, and GOCE satellites. For this study TOPEX/POSEIDON was chosen as the test satellite due to its well-verified precise orbits. The quality of the kinematic solution from TDs was assessed by comparing it to the well-verified MSODP dynamic solution.

2 GPS data pre-processing

The first step of the kinematic orbit determination approach is the GPS data pre-processing where the raw GPS data in RINEX format is processed in order to facilitate the later estimation process. This step corrects the receiver time tags, edits bad data, forms the ionospheric-free double-differenced (DD) observable, and sorts and merges the data sets. The DD observable involves two GPS satellites, one ground station, and one low-altitude user satellite. The data from the subset of the global GPS network of the International GPS Service for Geodynamics (IGS) were used to form the DD observables. Approximations of the unknown DD ambiguity terms are calculated and added to the DD observable during the pre-processing step. Thus a large portion of the DD ambiguity terms is corrected during this step. The GPS data pre-processing software system known as TEXGAP (the university of TEXas Gps Analysis Program) was established during the development of MSODP. It is currently implemented on a Unix workstation platform (Byun 1998). Since the kinematic orbit determination approach requires the TD as the main observable, one more step to form the TD is added to the pre-processing stage. The TD is easily generated by differencing the DD data between epochs.

3 TOPEX/POSEIDON GPS data

High-quality GPS orbits are needed for the kinematic precise orbit determination process. Precise GPS orbits are routinely calculated in dynamic mode by using the GPS observation data from a well-established network of IGS sites. For this research, the GPS data from TOPEX/POSEIDON and 24 IGS ground receivers on 24 April 1995 were used. Figure 1 shows the relatively uniform global distribution of the IGS stations used. There are nine fiducial sites which are shown as large squares. Their positions are known accurately by using other positioning methods, and are held fixed during the GPS orbit determination process. There are 15 regular ground stations which are shown as circles in Fig. 1. Their positions are not fixed during the GPS orbit determination process, but are estimated with the GPS orbit. These estimated regular ground-station positions are used for the kinematic orbit determination process where ground stations are always assumed fixed.

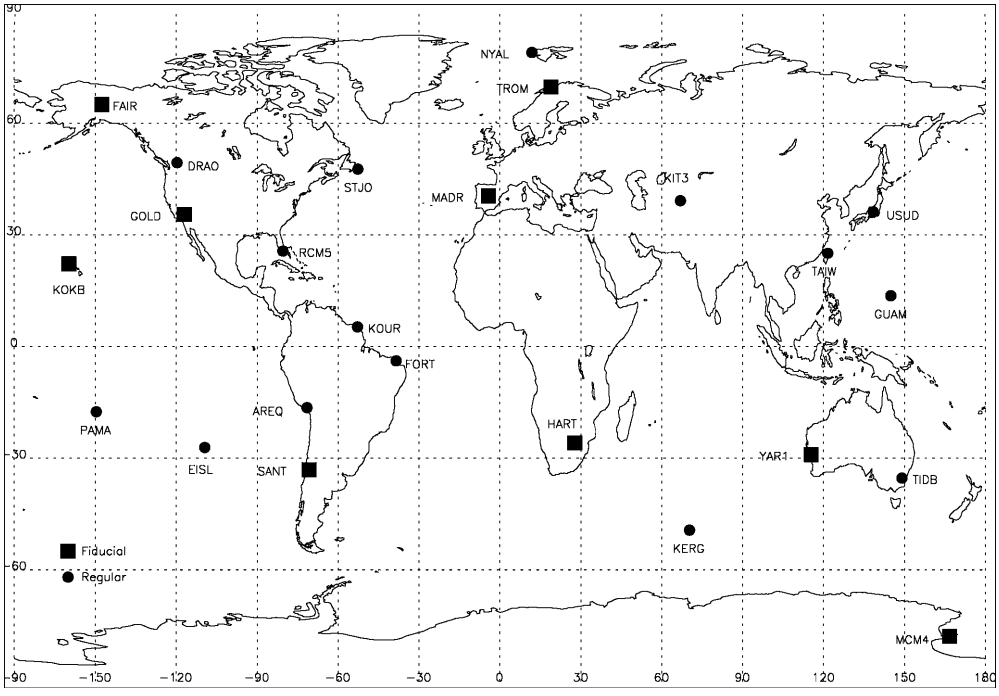

Fig. 1. Distribution of IGS-95 GPS tracking stations used for TOPEX/POSEIDON orbit determination

3.1 Quality and quantity assessment of differenced observables

In the case of the dynamic orbit determination approach, good-quality orbit solutions can be obtained at epochs with bad observations (or no observations at all) as long as the bad observations can be properly edited out and an accurate satellite dynamics model is available. This is possible since the satellite dynamics model can provide a continuous satellite state. Thus, the satellite state at an epoch without enough observations can be obtained from the observations at other epochs by using the satellite dynamics model.

However, in the case of the kinematic orbit determination approach, where the process depends entirely on the observation geometry, it is impossible to compute the satellite position at epochs without enough observations since the satellite positions at each epoch are independent parameters. Thus, the GPS data quality is very important in the kinematic orbit determination problem, and should be carefully checked before kinematic orbit determination is attempted. Figure 2 shows the number of TD observables at each epoch for one day, and a very similar plot can be obtained for DD observables. In Table 1, the second and the third column show the averages and the standard deviations of the numbers of DD/TD observables, respectively. The fourth column of Table 1 shows the maximum number of DD/TD observables occurring at an epoch near 16:00 hr. On average, there are about 15 DD/TD observations. However, as Fig. 2 shows, the number of the

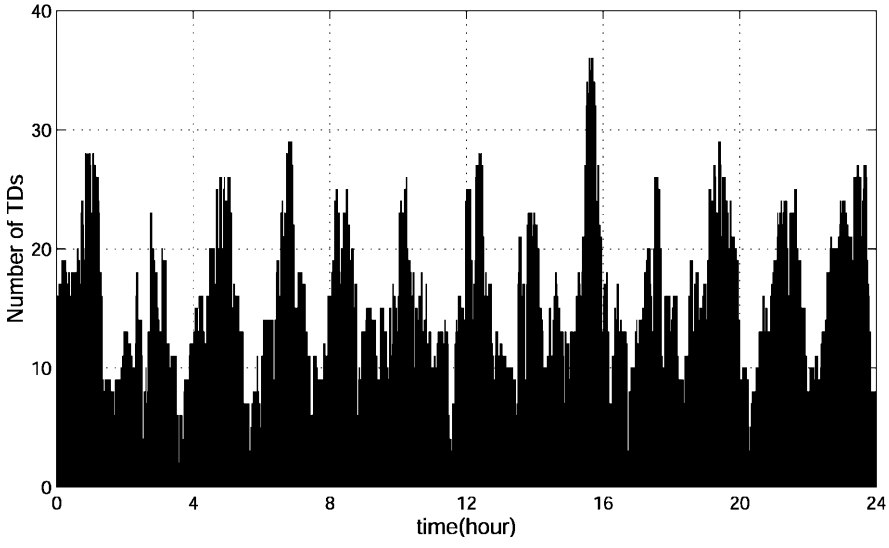

Fig. 2. Number of TDs for TOPEX/POSEIDON at each epoch (24 April 1995)

Table 1. Statistics for the number of DD and TD observables

Type	Mean	Standard deviation	Max
DD	15.57	6.22	37
TD	15.15	6.20	36

observables changes considerably during the course of one day. TOPEX/POSEIDON's on-board GPS receiver has six channels. If an on-board receiver was equipped with more channels, more DD/TD observables would be available.

For the computation of an a priori satellite position, the DD ambiguities are assumed to be known, and a minimum of at least three DD observations is required at each epoch (discussed later). Otherwise, the user satellite position cannot be calculated in the kinematic approach. In addition to the number of observations, good geometric distribution of the GPS satellites is required to compute reasonably accurate a priori positions. This is especially true when few DD observations are available. Table 2 shows the number of epochs with few DD/TD observations. The second column of Table 2 shows the number of epochs with three DD/TD observations or less; the third column shows the number of epochs with four observations or less, and so on. In theory, three DD observations are the minimum requirement for a priori user-satellite position computation. However, taking into consideration the geometric GPS satellite distribution and the possibility of bad DD observations, five DD observations are considered the minimum number of observations for this study. When an epoch with less than the minimum requirement of DD observations is encountered, the epoch is simply skipped.

Table 2. Number of epochs with few DD and TD observations

Type	≤ 3	≤ 4	≤ 5	≤ 6
DD	30	56	85	138
TD	38	71	106	168

When a sequential batch filter (described later) is used to process the TD data, a minimum number of six TD observations is required at each epoch. Considering the geometric GPS satellite distribution and the possibility of bad TD observations, seven TD observations are considered the minimum number of observations for this study. When an epoch with less than the minimum requirement of TD observations is encountered, the epoch is simply skipped for sequential batch filtering. Figure 3 shows the 168 epochs with six TD observations or less. This figure helps to identify which epochs to avoid when a sequential batch filter is used to process the TD data.

4 A priori orbit solutions

A large portion of the DD ambiguity values is calculated and added to the DD observations during the preprocessing stage. Thus, by assuming that the DD ambiguity is zero and all measurement errors including tropospheric delay have been corrected, the ionospheric-free DD observable can be written in simple form as:

$$DD_{ju}^{c\ pq}(t) = \rho_j^p(t_j) - \rho_u^p(t_u) - \rho_j^q(t_j) + \rho_u^q(t_u) \tag{1}$$

where

ρ = computed range with error corrections
p, q = GPS satellite identification numbers
j = j-th ground station receiver
u = user satellite
t = nominal epoch
t_j = corrected ground receiver time tag
t_u = corrected satellite receiver time tag

Since the GPS satellite ephemerides and the ground station positions are assumed to be known, the user satellite's position, $X(t) = [X_u(t) Y_u(t)\ Z_u(t)]^T$, at the nominal epoch t is the only unknown in the above

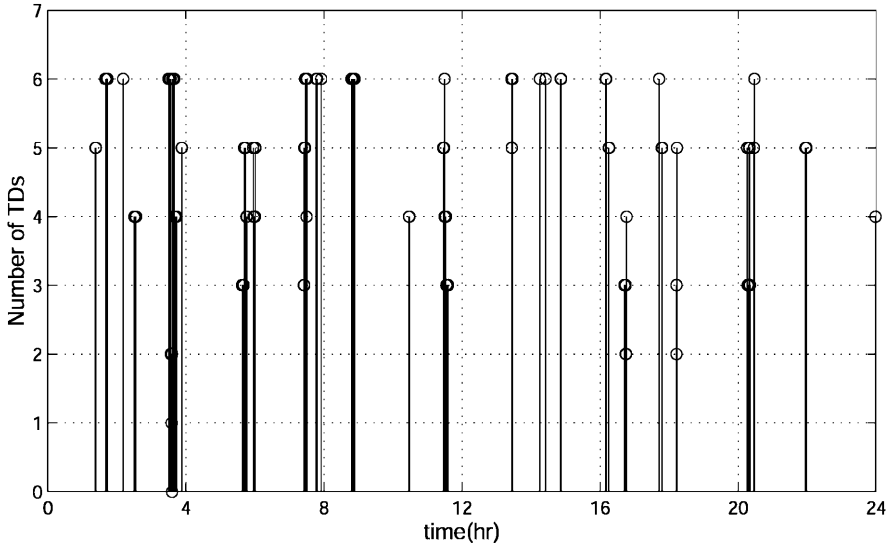

Fig. 3. Epochs with six TDs or less (24 April 1995)

equation. Assuming there is a sufficient number of DD observations at epoch t, the a priori satellite position, $X(t)$, is estimated by processing the DD data using an LS batch filter. Once a priori satellite positions are obtained for every epoch, a priori satellite velocities are computed by using a ninth-order polynomial interpolation of the position solutions (Remondi 1984). As discussed later, these a priori solutions are used during the first forward iteration using the sequential batch filter.

4.1 Singular value decomposition method

The LS method of directly inverting a normal matrix works fine as long as there is a sufficient number of good DD observations. However, this normal matrix is underdetermined at epochs with less than three DD observations. Sometimes, even at epochs with three or more DD observations, a poor distribution of GPS satellites can make the normal matrix very close to singular. Thus, directly inverting the normal matrix can fail or cause numerical instability, especially at the epochs with few DD observations. Therefore, instead of directly inverting the normal matrix, Singular value decomposition (SVD) method is employed for the computation of the a priori user satellite position. The SVD approach can be computationally extensive, and thus significantly slower than directly solving the normal equations. However, its great advantage is that SVD is numerically very stable, and it cannot fail, at least theoretically, even if the normal matrix is singular. SVD always provides a solution or some other useful information (Press et al. 1992).

In order to obtain a unique a priori solution, a minimum of three DD observations is needed at each epoch. Even though the SVD method can theoretically set a solution of an underdetermined problem at epochs with less than three DD observations, these epochs are simply skipped since SVD produces the mathematically smallest values (in the LS sense), which are not necessarily the correct ones. The SVD produces the best LS approximation for overdetermined epochs (Golub and Van Loan 1996). The quality of the solution can be checked later by examining the minimum of the singular values and the RMS of the measurement residuals.

4.2 A priori solution from DDs

In Fig. 4, the a priori solutions from the DD observations are compared to the MSODP solutions in the satellite-centered RTN (Radial–Transverse–Normal) coordinate system. Even though the figure does not show outliers, there are some epochs with orbit errors as large as several hundred meters. These are the epochs with few DD observations or with unfavorable GPS satellite distribution geometry. As long as there is a sufficient number of DD observations, a priori orbit solutions with less than 14 m total RMS orbit error can be obtained. Table 3 shows the means and the RMS of the orbit differences in RTN coordinates. Due to the ignored DD ambiguities, high values of the RMS about the means can be seen as expected. Even though the DD ambiguities are ignored for the computation of the a priori orbit solution, the quality of the a priori orbit accuracy increases with increasing number of observations. This is because when there are many DD observations at an epoch, the effect of the ignored ambiguities (some have positive values and some have negative values) can be averaged out and thus they more or less cancel with each other.

The a priori orbit is the solution of the three unknowns at each epoch in an LS sense. Since the SVD method is used for the LS problem, there are three singular values corresponding to the a priori solution at each epoch. Thus, the quality of the solution at each epoch can be assessed by examining the corresponding singular values, and it can be observed that the epochs with small singular values have few observations.

Figure 5 shows the differences between the a priori velocity computed by interpolating the a priori position solution and the MSODP velocity solutions in the RTN coordinate system excluding outliers. These a priori velocity solution outliers are caused by interpolating bad a priori positions. Note that even though the velocity error is at cm/sec level, it is acceptable for the kinematic orbit determination purpose where the velocity information is used only for the relativistic Doppler shift correction. In fact, this correction term is very small and can easily be ignored. Table 3 also shows the means and the RMS of the velocity differences.

5 Kinematic solutions from TDs

Satellite orbit determination using GPS-differenced observables in kinematic mode is quite different from the traditional dynamic approach. If satellite dynamics are used and the satellite initial state and the DD ambiguities are estimated along with the other force- and measurement-model-related parameters, the satellite orbit determination problem using the DD date is observable (solvable).

The problem becomes unobservable (underdetermined) if we try to estimate the satellite positions at every epoch and all of the DD ambiguities together in kinematic mode without any constraints. To avoid the unobservability, we can search for the unknown DD ambiguities starting from a priori solutions from the DDs. However, this ambiguity searching method is not practical when the DD ambiguities are real numbers instead of integers due to the huge ambiguity search space associated with real numbers. Even if constraints are provided for the DD ambiguities, there are so many parameters to be estimated in comparison to the number of observations that the estimation process could easily converge to the wrong local minimum (Byun and Schutz 2001).

In order to make the problem more tractable, the TD observable is used to improve the a priori solutions from

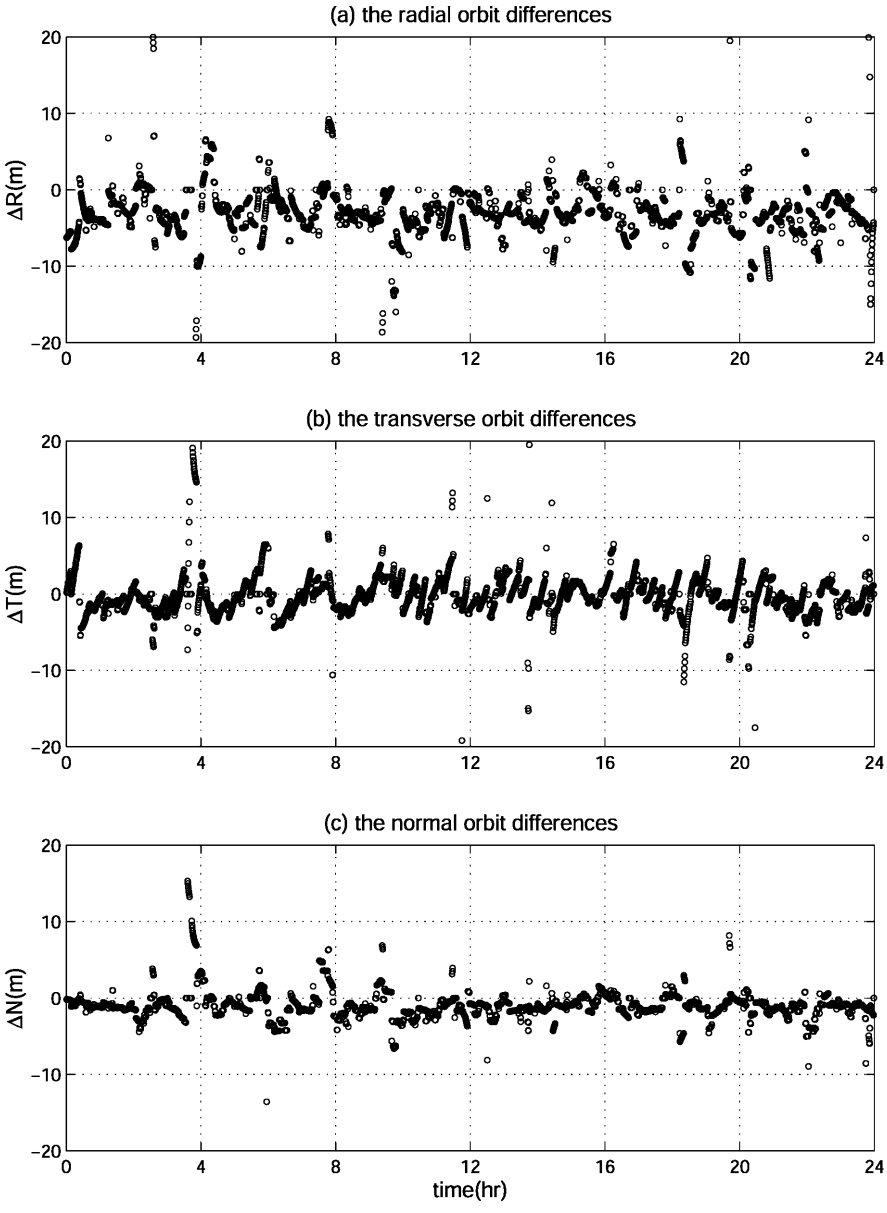

Fig. 4. Differences between the a priori and the MSODP orbit solutions

the DDs. Using the TDs, there are fewer observations than with the DDs. Furthermore, the TDs are noisier and more correlated with each other than the DDs. However, by processing the TD observables epoch by epoch, the kinematic orbit determination approach becomes observable, and it is possible to improve the satellite a priori position solution without using the satellite dynamics.

The kinematic orbit determination algorithm using the TD observables is composed of two steps: (1) sequential batch filtering and (2) multi-epoch batch filtering. The sequential batch filter is a hybrid filter having the properties of batch and Kalman filters. This filter is used first to improve the a priori orbit solution by filtering the TDs in both forward and backward directions. Then, the multi-epoch batch filter is used to smooth the outlying solutions, if any, and to estimate the position solutions at epochs skipped by the sequential batch filter.

It should be noted that the TD observable has relatively weak information since it is generated by differencing three times. In fact, it only contains information on position change since it is differenced between epochs. If we skip the sequential batch filtering and go straight to the multi-epoch batch filtering using the a priori solutions from DDs, the solutions may converge to local minimums instead of near true solutions due to the weak information content of TDs. Therefore, the sequential batch filtering is necessary and important.

Table 3. Statistics of differences between the a priori and the MSDOP orbit

Statistic	ΔR (m)	ΔT (m)	ΔN (m)	$\Delta\dot{R}$ (m/s)	$\Delta\dot{T}$ (m/s)	$\Delta\dot{N}$ (m/s)
Mean	−3.3892	−0.1224	−0.9445	−0.0003	−0.0001	0.0032
RMS	13.0746	5.2717	4.0477	0.1789	0.4149	0.1348

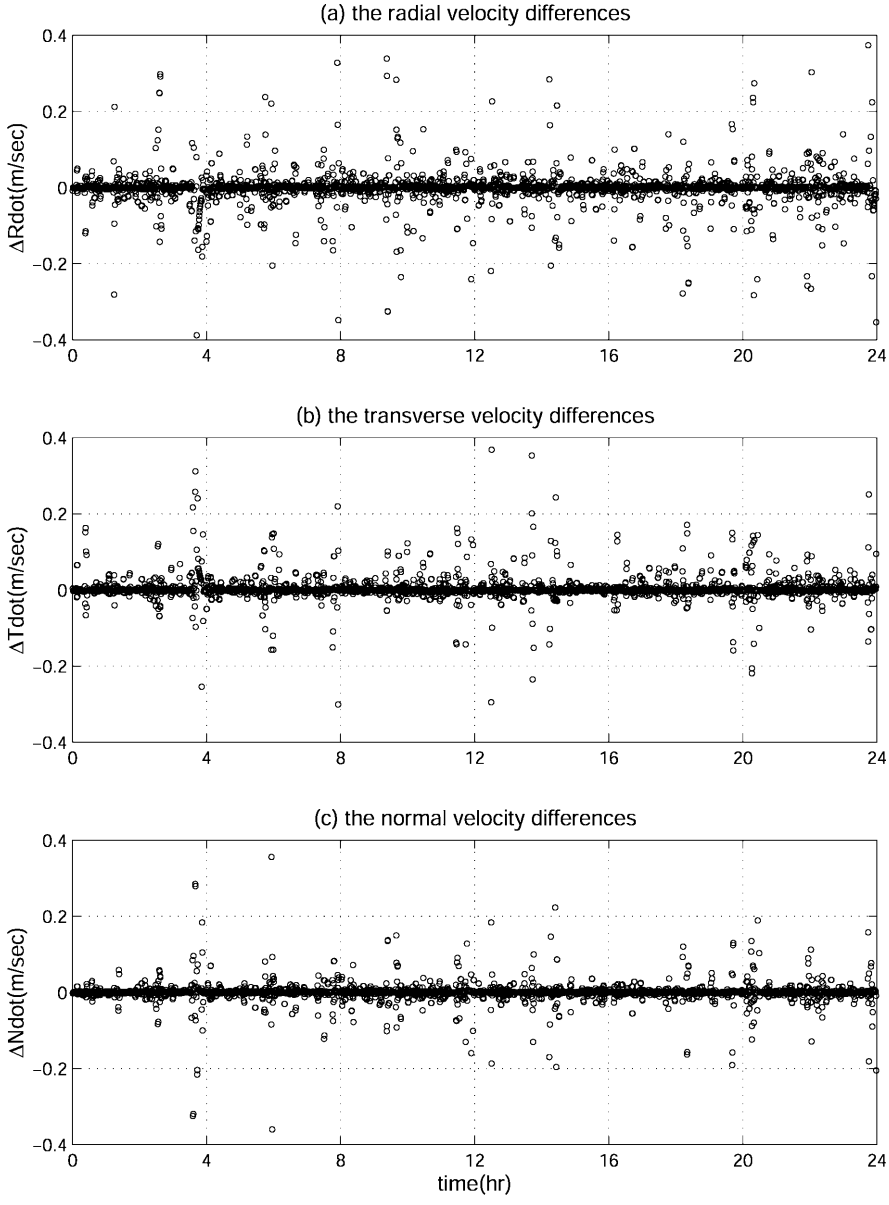

Fig. 5. Differences between the a priori and the MSODP velocity solutions

The TDs are correlated observables and taking into account the correlation will enhance the accuracy of an estimated orbit solution. However, the general decorrelation process requires the inverse of the measurement noise matrix whose size is the same as the number of observations at an epoch. Thus, considering the decorrelation process requires more computation time. Since two of the advantages of the kinematic approach are its simplicity and speed, two different cases are tested and compared: considering the TD data correlation, and not considering the correlation. In the case of the TOPEX/POSEIDON satellite, there is an unexplained radial direction antenna offset (6 cm) which can be empirically estimated when the dynamic approach is used (Bertiger et al. 1994). For the kinematic orbit determination approach, in order to investigate the effect of the antenna offset on the orbit solution, two more cases are tested: one without considering the antenna offset effect, and one with the antenna offset effect initially corrected.

By considering the decorrelation process and the antenna offset, the four test cases shown in Table 4 can be formed. The four cases are labeled sol0, sol1, sol2, and sol3, and will be used consistently in this article. Note that the sol0 case is expected to have the worst precision. The accuracy is expected to increase with increasing case number; the best solution is expected to be the sol3 case.

Table 4. The four test cases of kinematic orbit determination

Case	Decorrelation	Antenna offset
sol0	no	no
sol1	no	yes
sol2	yes	no
sol3	yes	yes

5.1 Sequential batch LS method

After all measurement corrections including tropospheric delay have been applied, the ionospheric-free TD observable can be written as

$$TD_{ju}^{c\,pq}(t_k) = \left[\rho_j^p(t_j) - \rho_u^p(t_u) - \rho_j^q(t_j) + \rho_u^q(t_u)\right]_{t_k} - \left[\rho_j^p(t_j) - \rho_u^p(t_u) - \rho_j^q(t_j) + \rho_u^q(t_u)\right]_{t_{k-1}} \quad (2)$$

where ρ is the computed range with error corrections, and all superscripts and subscripts are the same as for Eq. (1).

The TD observable has the user satellite's position information at the current epoch, t_k, and that at the previous epoch, t_{k-1}. However, this is the difference of DD observables at two epochs, and thus it has the information on the user satellite's position change between two epochs rather than the user satellite's absolute position information at two consecutive epochs. When a satellite dynamics model is used with the TD observable, the dynamic model can provide approximate information on the satellite's absolute position while the TD observable provides the satellite's position changes over time. As long as the dynamic model is accurate and enough TDs are available, an accurate satellite orbit can be obtained (Goad et al. 1996).

On the contrary, when a kinematic approach is used for a short-arc orbit determination and the positions at all epochs are solved simultaneously, a limited number of the TD observables alone cannot provide enough information to estimate the satellite's absolute position due to the relative nature of the TDs. The estimated solution can easily converge to any local minimum instead of the best orbit solution. If a long arc covering more than one orbit revolution is considered, the TD observable alone may provide enough information for satellite orbit determination. Unlike in the dynamic approach, the position at each epoch is treated as an unknown independent parameter in the kinematic approach. Thus considering a very long arc is not practical due to the excessively large number of parameters to be estimated.

Nevertheless, it is possible to obtain a much improved orbit from the TDs with the kinematic approach by using an a priori orbit solution from the DDs and providing a proper a priori constraint. To implement this, a sequential batch LS filter was developed to process the TDs sequentially one epoch at a time in a batch mode.

5.1.1 Formulation

Since the TD observable has the user-satellite position information at two epochs, two proper time tags should be specified to distinguish the current epoch from the previous epoch in the formulation. By assuming that the GPS satellite orbit and ground station positions are known and all measurement corrections are properly applied, the user satellite's positions at the two epochs t_{k-1} and t_k

$$X(t_k) = [X_u(t_{k-1})Y_u(t_{k-1})Z_u(t_{k-1})X_u(t_k)\ Y_u(t_k)\ Z_u(t_k)]^T \quad (3)$$

are the only unknowns in Eq. (2). Assuming there are l TD observations available at epoch t_k, the ith measurement equation can be written as

$$Y_i(t_k) = G_i(X^*, t_k) + \varepsilon_i, \quad i = 1, 2, \ldots, l \quad (4)$$

where

$$G_i(X^*, t_k) = TD_{ju}^{c\,pq}(t_k) \quad (5)$$

X^* is the nominal value of X in Eq. (3), and ε_i includes measurement noise and all errors in parameters used to compute ρ. The linearized ith TD observation equation can be written as

$$y_i(t_k) = \tilde{H}_i x(t_k) + \varepsilon_i \quad (6)$$

where the observation state mapping matrix is

$$\tilde{H}_i = \frac{\partial G_i(X^*, t_k)}{\partial X} \quad (7)$$

and the error ε_i includes the linearization contribution. When the dynamic orbit determination approach is used, the mapping matrix $\tilde{H}_i$ is usually propagated to the reference epoch t_0 by using a state transition matrix $\Phi(t_0, t_k)$ as

$$H_i = \tilde{H}_i \Phi(t_0, t_k) \quad (8)$$

In the case of the kinematic orbit determination approach, the Φ matrix becomes an identity matrix since there are no satellite dynamics involved. Thus, the mapping matrix H_i is the same as $\tilde{H}_i$. By using the mapping matrix H_i and by adopting vector and matrix notations, Eq. (6) can be written as

$$y(t_k) = Hx(t_k) + \varepsilon \quad (9)$$

Here, the dimension of y is $l \times 1$; the dimension of H is $l \times 6$; the dimension of x is 6×1; and the dimension of ε is $l \times 1$. Assuming there are at least six or more TD observations at epoch t_k, the deviation vector, x, can be estimated by the LS method with a priori information as

$$\hat{\boldsymbol{x}} = (H^T R^{-1} H + \bar{P}^{-1})^{-1}(H^T R^{-1} y + \bar{P}^{-1}\bar{\boldsymbol{x}}) \quad (10)$$

where R is a measurement noise matrix, $\bar{P}$ is the a priori covariance of the user satellite position, and $\bar{x}$ is the a priori value of x as given below (Tapely 1973). When the TD data correlation is not considered, R is a simple diagonal matrix. However, this matrix becomes non-diagonal when the TD data correlation is considered. Since only two consecutive epochs are considered at a time in the sequential batch filter, the correlation matrix has only the correlation component due to the double-differencing process and not the correlation component due to the differencing in time. In other words, the correlation matrix for the sequential batch filter is a block diagonal matrix rather than a banded matrix.

The a priori covariance matrix, $\bar{P}$, can be written as

$$\bar{P}(t_k) = \begin{pmatrix} \bar{P}_{11}(t_k) & \bar{P}_{12}(t_k) \\ \bar{P}_{21}(t_k) & \bar{P}_{22}(t_k) \end{pmatrix} \tag{11}$$

where the subscript 1 denotes the satellite position at the previous epoch, t_{k-1}, and the subscript 2 denotes the satellite position at the current epoch, t_k. By processing the TD observables, the satellite positions at two consecutive epochs are estimated simultaneously. In order to overcome the weak information content of the TD data, the a priori position solution for the previous epoch is properly constrained by uncertainties of the a priori solution while the a priori solution of the current position is barely constrained. The a priori covariance matrix at the current epoch, t_k, is assigned as

$$\begin{aligned} \bar{P}_{11}(t_k) &\Leftarrow P_{22}(t_{k-1}) \\ \bar{P}_{12}(t_k) &\Leftarrow 0 \\ \bar{P}_{21}(t_k) &\Leftarrow 0 \\ \bar{P}_{22}(t_k) &\Leftarrow \sigma_2 I \end{aligned} \tag{12}$$

P_{22} is the a posteriori position covariance matrix solution at the previous epoch. In other words, the covariance matrix of the user satellite position at epoch t_{k-1} computed from the TD data at the epoch t_{k-1} is used as the a priori covariance matrix of the satellite position at the same epoch, t_{k-1}, when the TD data at epoch t_k are processed. At the initial epoch, the diagonal elements of submatrix $\bar{P}_{11}$ are assigned the values of the assumed error of the a priori satellite position from the DD observables. All elements of submatrices $\bar{P}_{12}$ and $\bar{P}_{21}$ are always set to zero. For the diagonal elements of submatrix $\bar{P}_{22}$, a very high value (no constraint), σ_2, is assigned; all other elements of $\bar{P}_{22}$ are set to zero.

The a priori position deviation, $\bar{x}$, at epoch t_k can be written as

$$\bar{x}(t_k) = \begin{pmatrix} \bar{x}_1(t_k) \\ \bar{x}_2(t_k) \end{pmatrix} \tag{13}$$

where the subscript 1 denotes the satellite position at the previous epoch, t_{k-1}, and the subscript 2 denotes the satellite position at the current epoch, t_k. The value of $\bar{x}$ at epoch t_k is assigned as

$$\begin{aligned} \bar{x}_1(t_k) &\Leftarrow \hat{x}_2(t_{k-1}) \\ \bar{x}_2(t_k) &\Leftarrow 0 \end{aligned} \tag{14}$$

where $\hat{x}_2$ is the a posteriori position deviation estimation at the previous epoch. At the initial epoch, $\bar{x}_1$ is set to zero. $\bar{x}_2$ is always set to zero. Thus, the updated satellite position at the previous epoch and the position at the current epoch, t_k, can be computed as

$$X(t_k) = X^*(t_k) + \hat{x}(t_k) \tag{15}$$

These updated satellite positions at two consecutive epochs are the re-adjusted position of the previous epoch and the newly updated position of the current epoch.

So far only the TD data from one epoch have been processed and only the satellite positions at two epochs have been updated. Due to the limited information of the TD observable, the estimated position solution at the current epoch may not be very accurate. However, the updated position is slightly better than its a priori position solution due to the added information from the TDs at the epoch t_k. The filter then propagates the solution to the next epoch, t_{k+1}, by using Eqs. (12) and (14). Then, the TD data at the epoch t_{k+1} are processed. This same process is repeated at each successive epoch until the final epoch is reached. As long as the TD data quality is consistently good, the satellite position solutions at the later epochs are more accurate as additional TDs are processed during the first forward filtering; thus the best estimated position may be obtained at the final epoch. While the estimated position at the final epoch is probably the best one, the estimated position at the initial epoch is probably the worst one.

Because the filter is running in post-processing mode, it is possible to process the TD data in reverse. A backward filter was developed to propagate the better solution at the final epoch to the proceeding epochs and thus to improve the quality of the solution throughout the whole data span. While the forward filter uses the TD observable

$$TD(t_k) = DD(t_k) - DD(t_{k-1}) \tag{16}$$

the backward filter uses the negative of the TD observable,

$$-TD(t_k) = DD(t_{k-1}) - DD(t_k). \tag{17}$$

When the filter runs in the backward direction, the position solutions from the previous forward filtering are used as the new a priori position information and the TD data are processed until the initial epoch is reached. Then the forward filter is applied again using the improved position solution from backward filtering as the new a priori value, and so on. This forward and backward filter combination (smoother) is used iteratively until the best solution from the TD data is obtained at all epochs.

When the user-satellite velocity information is needed, the a priori satellite velocities from the DD data are used during the first forward filtering. After processing with the forward filter, the satellite velocity is updated by polynomial interpolation of the updated satellite position. This velocity is used during the first backward filtering. Once the initial epoch is reached, the satellite velocity is updated by interpolating the updated satellite position solution from the backward filter. In the next forward iteration, the velocity solution from the last backward filtering is used, and so on.

5.1.2 Results from the sequential-batch filter

Since the TD observable has only the information on the satellite position change between two epochs, the final estimated position solution accuracy depends on how many epochs of TD data are processed (the time interval

between two consecutive epochs of the TD data is 30 sec in this study). Therefore, the sequential batch filter solution accuracy with respect to the amount of the TD data processed is investigated. The accuracy comparison of the solutions from 20, 30, 60, 90, 120, and 150 epochs of TD data is shown in Fig. 6 for the sol1 case. Figure 6 shows the orbit differences between the kinematic solution from the final forward filtering of the sequential batch filter and the MSODP orbit solution. In Fig. 6, the length of the plotted line indicates the amount of data processed. When the data length is short (20 or 30 epochs), the solution has a large radial orbit error of about 1 m. When a small amount of TD data is processed, the measurement residuals are fairly small but the orbit errors are large. This indicates that the solution has converged to the local minimum rather than the best orbit solution.

As the number of data epochs increases to 60, the estimated solution improves considerably. As the number of epochs increases further, the solution accuracy improves; however, considering more than 90 epochs of TD data fails to show any noticeable improvement. For this research, in order to make the book-keeping easy, 120 epochs of the TD data, which are equivalent to 1 hr, are considered at a time.

Table 5 summarizes Fig. 6 by showing the orbit differences in RMS for sol1 case, and Table 6 summarizes similar information for the backward filtering. For this particular time period, the backward filter solution is slightly less accurate than the forward filter when more than 90 epochs of the TD data are considered. However, the sequential batch filter alone cannot determine whether the forward solution or the backward solution is better. In general, the backward filter shows smaller values for the measurement residuals. However, a smaller residual does not necessarily mean a better orbit solution.

Figure 7 shows the convergence trends of the sequential batch filter during the iterations in the forward

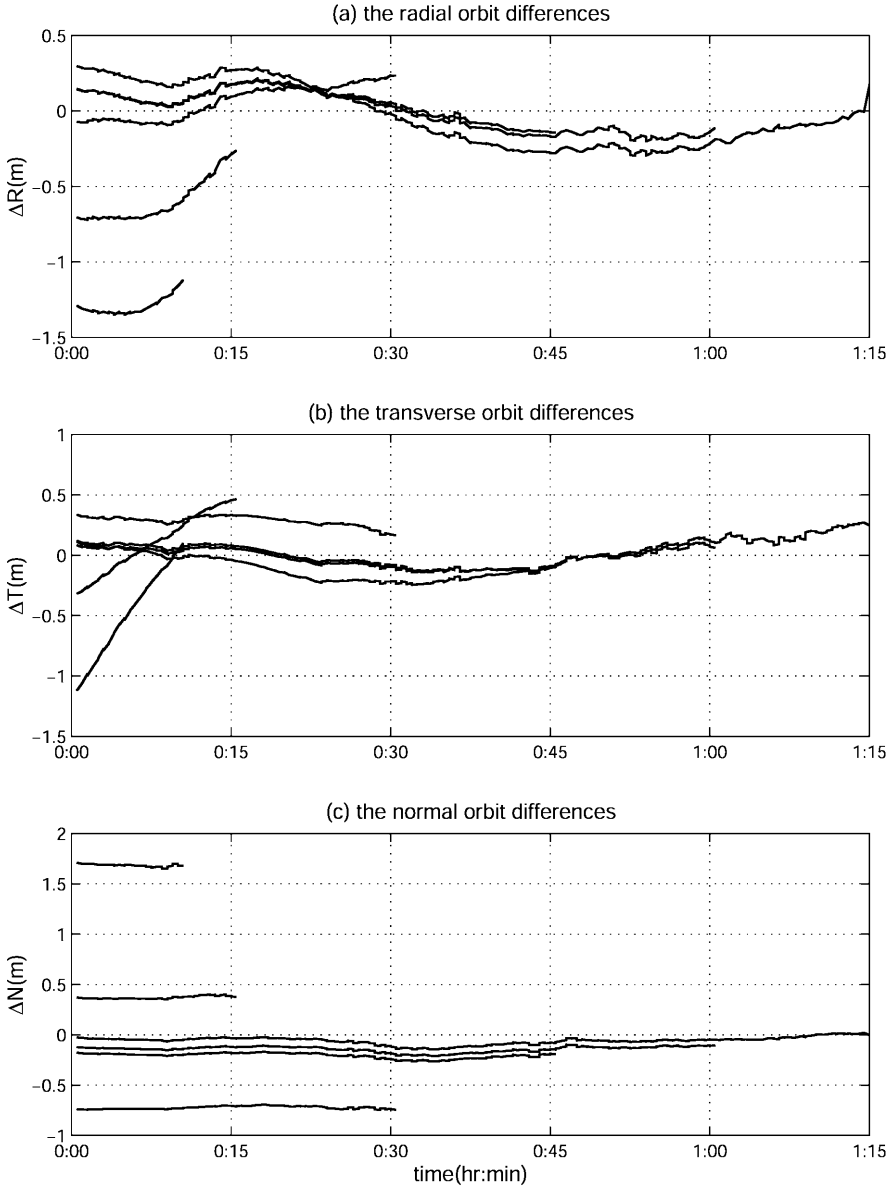

Fig. 6. Effect of the amount of TDs on the orbit accuracy from the sequential batch filter (sol1, forward)

Table 5. Effect of the amount of TDs on the orbit solution accuracy RMS from the sequential batch filter (sol1, forward)

No. epochs	ΔR (m)	ΔT (m)	ΔN (m)	Total (m)
20	1.2951	0.5984	1.6845	2.2075
30	0.6163	0.2604	0.3710	0.7651
60	0.1277	0.2884	0.7233	0.7891
90	0.1162	0.0892	0.2084	0.2547
120	0.1294	0.0776	0.1422	0.2087
150	0.2042	0.1463	0.0680	0.2603

Table 6. Effect of the amount of TDs on the orbit solution accuracy from the sequential batch filter (sol1, backward)

No. epochs	ΔR (m)	ΔT (m)	ΔN (m)	Total (m)
20	1.2742	0.5822	1.7009	2.2035
30	0.5931	0.2586	0.3559	0.7385
60	0.1254	0.2732	0.7327	0.7919
90	0.1501	0.1507	0.1679	0.2709
120	0.1515	0.1383	0.1146	0.2350
150	0.2788	0.2545	0.0328	0.3789

and backward directions. This figure shows the differences between the sequential batch filter solutions and the MSODP solution for the sol1 case. For these plots, 120 epochs of the TD data are used. At the initial epoch, the position uncertainty is given as 6 m, and a very large value is given for the position uncertainty at the current epoch. By using the kth-epoch TD observations, the filter can estimate the positions at the $(k-1)$th epoch and at the current kth-epoch together. The kth-epoch position is estimated again when the $(k+1)$th-epoch TDs are processed. Thus, there are always dual-position solutions at each epoch except at the initial and final epochs. This dual-position solution character can be seen as vertical lines in all three plots of Fig. 7. A very similar statement can be made for the filtering in the backward direction. Thus, there exist four different position solutions when the sequential batch filter is used with the TD data in the forward and backward directions. As shown in Fig. 7, the first iteration in the forward direction contributes the most to the solution convergence, while the following filtering in the backward direction does most of the solution smoothing. After four more iterations in the forward and backward directions, the solution converges.

Figure 8 is basically the same as Fig. 7, except that the first iteration in the forward direction is omitted. In Fig. 8, the light lines denote the filtering in the forward direction, and the dark lines denote the filtering in the backward direction. The solutions from filtering in the forward and backward directions get closer as the iteration number increases. However, after a certain point, they do not get any closer. The sequential batch filter finds the position solutions of two epochs at a time using the covariance information from the previous epoch solution. Unfortunately, the TD observations do not necessarily have the same quality throughout the entire data span. A different data quality at one epoch can result in a different covariance value, which then affects the solution quality of the next epoch. In other words, the quality of the TD data can push the position solution in a certain direction that is dependent on the sequence of the TD data. Therefore, the position solution from filtering in the forward direction is not necessarily the same as the solution from filtering in the backward direction. These four position solutions are passed to the next stage: the multi-epoch batch filter.

So far the results are for the case considering the antenna offset correction but not the TD observation correlation (sol1). Other cases were tested and Table 7 shows the orbit differences in RMS with respect to the MSODP dynamic solution for all four cases in Table 4. All cases used 120 epochs of the TD data. It is well known that the dynamic orbit solution is the most accurate in the radial direction. Thus, when assessing the accuracy of the kinematic orbit solutions with respect to the dynamic solution, more emphasis should be given to the radial component. As expected, the worst solution is for the sol0 case, and solutions improve as the sol1 and sol2 cases are processed. Finally, the best kinematic solution is obtained for the sol3 case. It should be noted that consideration of the observation decorrelation process is more important than consideration of the antenna offset in achieving more accuracy.

5.2. Multi-epoch batch LS method

At each epoch there are four separate position solutions from the sequential batch filter: two from the forward filtering and two from the backward filtering. Instead of selecting one of the solutions, a new batch filter, the multi-epoch batch filter, was developed to estimate the position at every epoch simultaneously by processing the TD data. The sequential batch filter solutions are used as the a priori information.

When the quality of the solution from the sequential batch filter is good, the multi-epoch batch filter only marginally improves the sequential batch filter solution. However, when there are outliers in the solution from the previous step, the multi-epoch batch filter can smooth out the bad position solution by considering the whole data set simultaneously.

There is another useful application of the multi-epoch batch filter. In the case of the sequential batch filter, two position solutions are estimated at each epoch. Thus, a minimum of six TD observations is required at every epoch. However, as shown in Fig. 3, there are many epochs with less than six TD observations, and the sequential batch filter cannot continuously process the data from these epochs. In the case of the multi-epoch batch filter, which estimates only one position solution at each epoch, a minimum of three TD observations is required at every epoch. Thus, when an epoch has less than six but more than three TD observations, the epoch can be processed by the multi-epoch batch filter. For example, assume that there are more than six TD observations at all epochs except at epoch t_k, where the

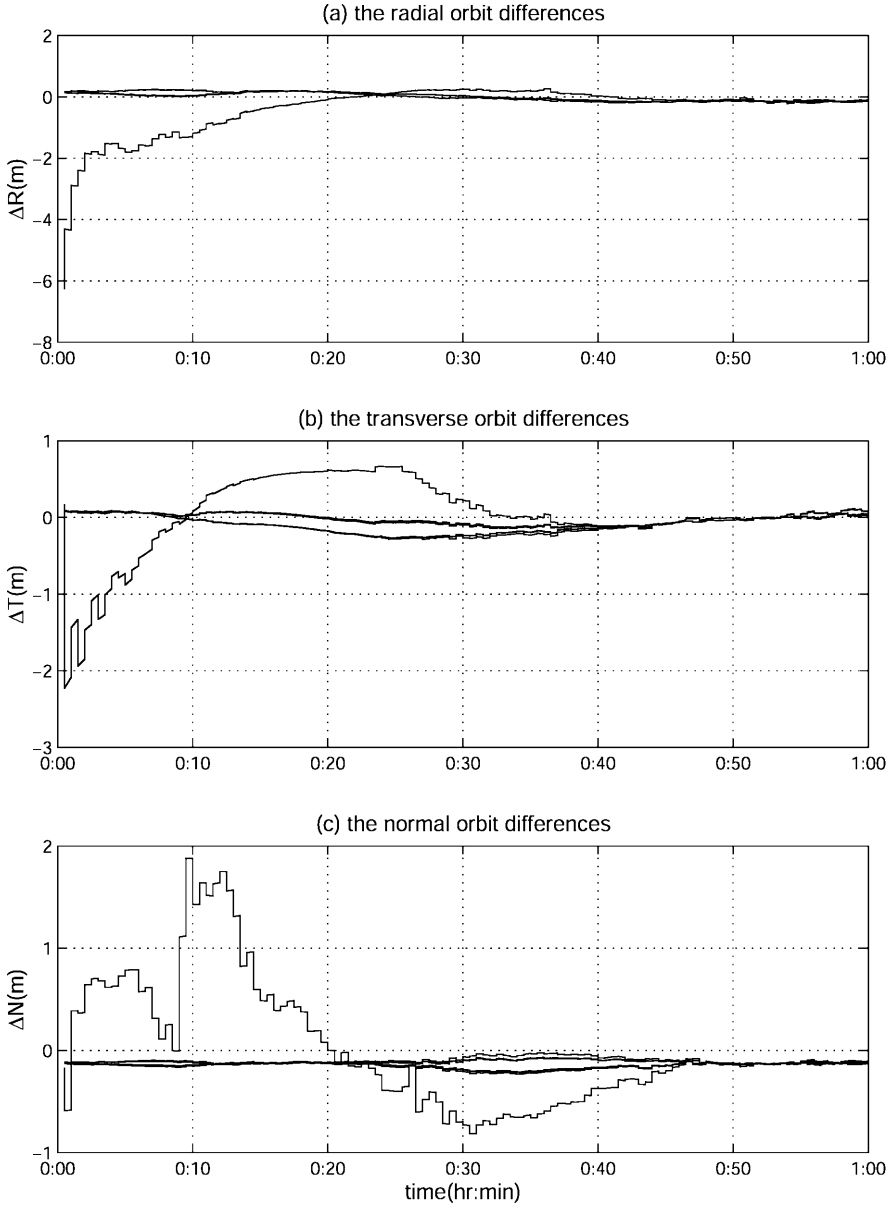

Fig. 7. Convergence character of the sequential batch filter (sol1)

number of TD observation is less than six but more than three. Skipping epoch t_k, the TD data can be divided into two parts: one part starting from epoch t_0 and ending at epoch t_{k-1}, and the other part from epoch t_{k+1} to final epoch t_f. These two data sets can be processed separately by the sequential batch filter. Then, the entire TD data including epoch t_k can be processed using the multi-epoch batch filter. The solution from the sequential batch filter is used as the a priori position at all epochs except epoch t_k, where the previous a priori position solution and covariance from the DD data processing are used instead.

5.2.1 Formulation

The formulation for the multi-epoch batch filter is similar to that for the sequential batch filter. The only difference is that while only two positions are estimated at a time by the sequential batch filter, all positions are estimated simultaneously by the multi-epoch batch filter. The position vector of Eq. (3) now becomes,

$$X = [X_0\, Y_0\, Z_0\, X_1\, Y_1\, Z_1\, \cdots\, X_n\, Y_n\, Z_n]^T \tag{18}$$

where the subscripts 0 and n denote the initial and final epochs, respectively. When n epochs of TD data are considered, the vector size becomes $(n+1)\times 3$, since each position is independent with respect to any other position and must be estimated as a separate parameter. As the amount of data increases, the size of the position vector increases. For this reason, the TD data size to be processed at any one time should be limited. For the multi-epoch batch filter, the same 1-hr TD data processed by the sequential batch filter are used.

Assuming there are l TD observations throughout n epochs, the ith measurement equation can be written as

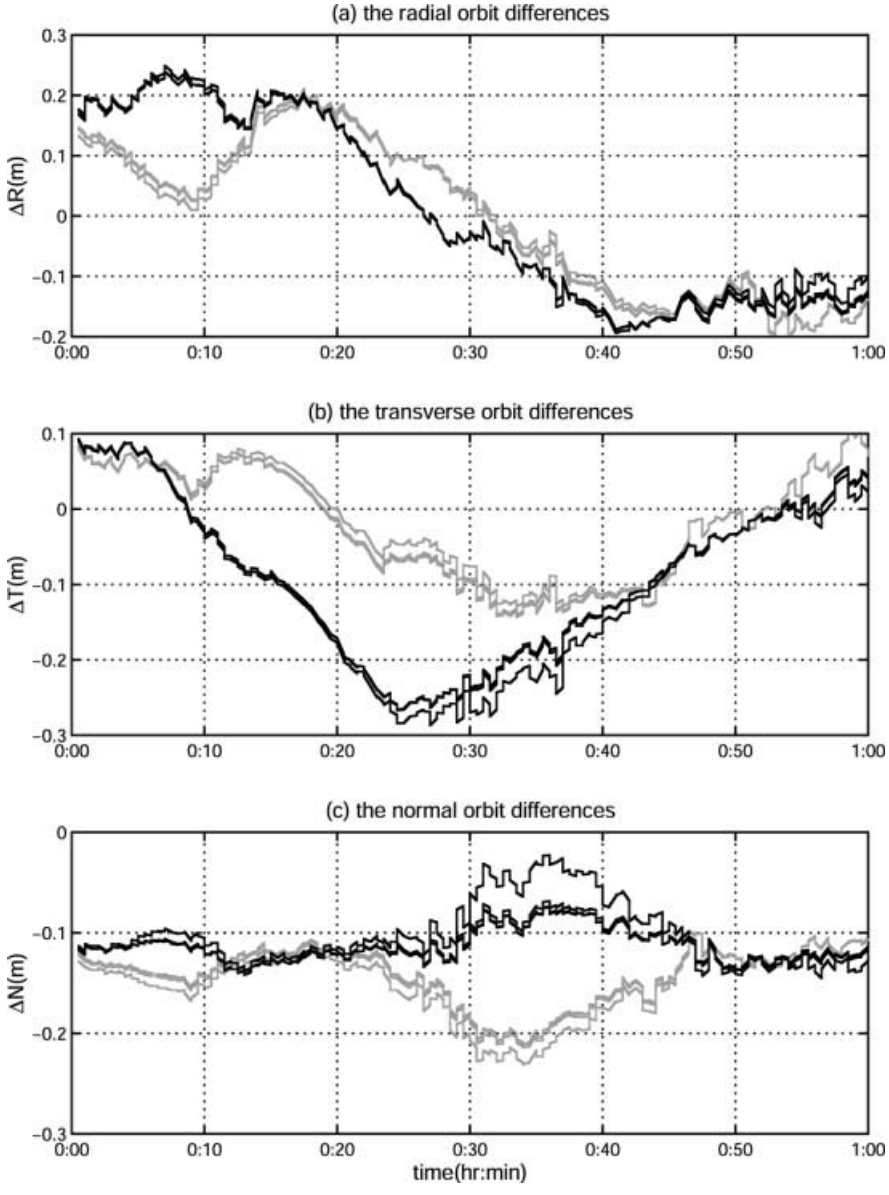

Fig. 8. Convergence character of the sequential batch filter after the first iteration (sol1). *Dark color* denotes forward iteration and *light color* denotes backward iteration

$$Y_i(t) = G_i(X^*, t) + \varepsilon_i, \quad i = 1, 2, \ldots, l \tag{19}$$

where

$$G_i(X^*, t) = TD_{ju}^{c\,pq}(t) \tag{20}$$

X^* is the nominal value of X from the sequential batch filter, and ε_i includes measurement noise and all errors in parameters used to compute ρ. The ith computed observation G_i is only a function of the satellite positions at the previous and current epochs within the position vector, X. By following a similar derivation to that of the sequential batch filter case, the linearized ith TD observation equation can be written as

$$y_i = \tilde{H}_i x + \varepsilon_i \tag{21}$$

where the observation state mapping matrix is

$$\tilde{H}_i = \frac{\partial G_i(X^*, t)}{\partial X} \tag{22}$$

and the error ε_i includes the linearization contribution. Since G_i is a function of the position vector, X, Eq. (22) can be rewritten as

$$\frac{\partial G_i}{\partial X} = \left[\frac{\partial G_i}{\partial X_0}\frac{\partial G_i}{\partial Y_0}\frac{\partial G_i}{\partial Z_0}\frac{\partial G_i}{\partial X_1}\frac{\partial G_i}{\partial Y_1}\frac{\partial G_i}{\partial Z_1}\cdots\frac{\partial G_i}{\partial X_n}\frac{\partial G_i}{\partial Y_n}\frac{\partial G_i}{\partial Z_n}\right] \tag{23}$$

Only six elements in this vector, which correspond to the positions at the current and previous epochs, are non-zero; all other elements are zero. Since there are no satellite dynamics, the mapping matrix, $\tilde{H}_i$, is the same as H_i as in the formulation of sequential batch filter. In matrix notation, the linearized observation equations can be written as

$$y = Hx + \varepsilon \tag{24}$$

where the dimension of the y vector is $l \times 1$; the dimension of the H matrix is $l \times 3(n+1)$; the dimension

Table 7. RMS of differences between the sequential batch filter and the MSODP orbit solutions: final iterations

Case	Direction	ΔR (m)	ΔT (m)	ΔN (m)	Total (m)
sol0	fwd	0.1387	0.0766	0.1442	0.2146
	bwd	0.1626	0.1383	0.1146	0.2422
sol1	fwd	0.1294	0.0776	0.1442	0.2087
	bwd	0.1515	0.1383	0.1146	0.2350
sol2	fwd	0.1157	0.0832	0.2551	0.2922
	bwd	0.0968	0.0436	0.2312	0.2545
sol3	fwd	0.0828	0.0832	0.2551	0.2809
	bwd	0.0482	0.0437	0.2312	0.2402

of the x vector is $3(n+1) \times 1$; and the dimension of the ε vector is $l \times 1$. Assuming there are at least three observations at every epoch, the deviation vector, x, of dimension $3(n+1) \times 1$ can be estimated by

$$\hat{x} = (H^T R^{-1} H + \bar{P}^{-1})^{-1} (H^T R^{-1} y + \bar{P}^{-1} \bar{x}) \tag{25}$$

where R is a measurement noise matrix, $\bar{P}$ is an a priori position covariance of the user satellite, and $\bar{x}$ is an a priori value of x (Tapley 1973). All a priori values are from the sequential batch filter solution, except the values at the epochs with less than six TD observations. The previous a priori solutions from the DD processing are used instead at these epochs.

The application of Eq. (25) to a real-world problem, however, requires some other considerations. When the TD data from many epochs are processed simultaneously, the row dimension of the H matrix, and the row and column dimension of the R matrix, are the same as the total number of TD observations. This number can easily reach several thousand with only half an hour of actual TD data. Thus, the straightforward formulation of Eq. (25) involving the inverse R matrix is not practical for computer programming, especially when the TD observation decorrelation process is considered.

5.2.2 Correlated differenced observation data

The undifferenced and single-differenced GPS phase measurements are assumed not to be correlated. Thus the associate R matrices are simple diagonal matrices, and their inverses are obtained simply by replacing each element with its reciprocal. However, DD phase measurements are correlated by sharing common GPS satellites and receiving antennas (Hofmann-Wellenhof et al. 2001). When n epochs of DD data are processed simultaneously, the double-differencing coefficient matrix can be written as

$$D = \begin{bmatrix} D_1 & & & \\ & D_2 & & \\ & & \ddots & \\ & & & D_n \end{bmatrix} \tag{26}$$

where each D_k is the double-differencing coefficient matrix for the kth epoch. The DD cofactor matrix is formed by multiplying the double-differencing coefficient matrix with its transpose. Then the measurement noise matrix is formed by

$$R = DD^T \sigma \tag{27}$$

where σ is the measurement noise of the GPS carrier phase (Leick 1995). This correlated measurement noise matrix, R, is a block diagonal matrix as follows

$$R = \begin{bmatrix} R_1 & & & \\ & R_2 & & \\ & & \ddots & \\ & & & R_n \end{bmatrix} \tag{28}$$

and there is no correlation between epochs. The inverse of the R matrix can be computed by inverting each individual diagonal submatrix independently as (Brogen 1991)

$$R^{-1} = \begin{bmatrix} R_1^{-1} & & & \\ & R_2^{-1} & & \\ & & \ddots & \\ & & & R_n^{-1} \end{bmatrix} \tag{29}$$

The TD observations are correlated not only by sharing the common GPS satellites and a ground station, but also by sharing the same epoch, because of the between-epoch differencing. The TD cofactor matrix is formed by multiplying the triple-differencing coefficient matrix with its transpose. This matrix is a banded matrix with a profile that depends on the way the triple differences are built. Figure 9 shows the banded TD cofactor matrix formed from the initial four epochs of the TOPEX/POSEIDON TD data on 24 April 1995. In Fig. 9, the horizontal axis denotes the column index of the matrix; the vertical axis denotes the row index of the matrix; each dot denotes any non-zero element in the matrix. The inverse of this banded cofactor matrix may be a full matrix. Golub and Van Loan (1996) described a detailed mathematical treatment of a banded matrix.

Since numerous observations are involved in the satellite orbit determination problem, the size of the TD cofactor matrix can be very large. Due to the size and the banded shape of this matrix, it is very difficult or even impossible to handle the matrix by using the standard matrix inversion procedure. Thus, a different decorrelation scheme employing the right-looking Cholesky factorization of the TD cofactor matrix is applied. This method eliminates the need for the inverse of the TD cofactor matrix by using a forward substitution scheme for the normal equation. Also, by using the property of a banded matrix, the computation is substantially more efficient. Since R is a matrix resulting from the correlation of two consecutive epochs, only two epochs of the TD data need to be considered simultaneously. The description of the recursive Cholesky decomposition, and the decorrelation scheme operating on the lower triangular part of the original TD cofactor matrix, R, can be found in the paper by Goad et al. (1996).

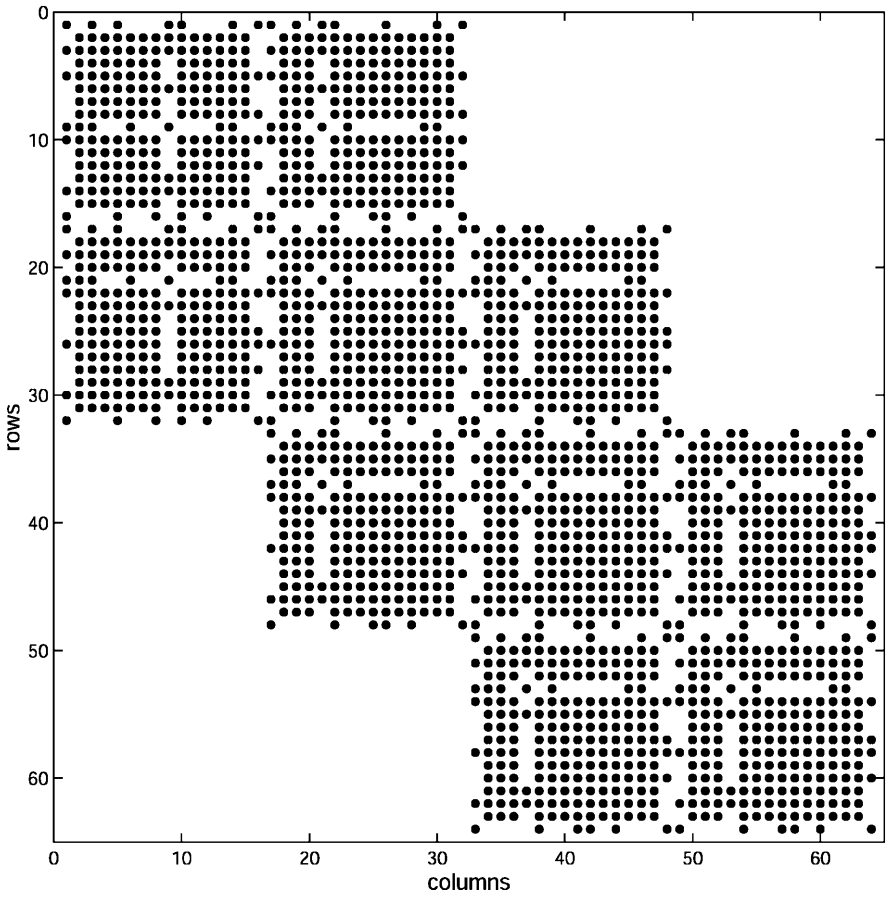

Fig. 9. Shape of the banded TD cofactor matrix from four consecutive epochs. There are 2020 non-zero elements

5.2.3 Results from the multi-epoch batch filter

Figure 10 shows the differences between the multi-epoch batch filter solution and the MSODP solution for the sol0 case. Figure 10 also shows the differences between the sequential batch filter solution and the MSODP solution for the same case. When the TD data are processed in the sequential batch filter, four separate position solutions, two from the forward filtering and the two from the backward filtering, are obtained. The crosses indicate the results from filtering in the forward direction, and the circles indicate the results from filtering in the backward direction. The light solid lines denote the results from the multi-epoch batch filter using the forward a priori value from the sequential batch filter, while the dark solid lines denote the results from the multi-epoch batch filter using the backward a priori values.

Table 8 shows the orbit differences in RMS between the multi-epoch batch filter and the MSODP solution for all four cases. By comparing Table 8 with Table 7, it can be seen that the orbit improvement achieved by the multi-epoch batch filter is marginal for all four cases. Using the multi-epoch batch filter cannot greatly improve the orbit over that with the sequential batch filter when the same TD data are processed. The multi-epoch batch filter uses the position solution from the sequential filter as a priori information. By using this a priori value, the measurement residuals are already small and do not contain much information for position solution improvement. However, the multi-epoch batch filter can smooth out outliers, and is also important when there are epochs with less than six TD observations but more than three. In this case the multi-epoch batch filter allows continuous filtering of the data through epochs with few observations.

After the multi-epoch batch filtering, we end up with two position solutions: forward solution and backward solution. Even though more study is required to determine which one is better in general, it is believed that the difference between the forward and backward solutions is probably the accuracy limit of the position solutions from the kinematic approach using TDs (Byun and Schutz 2001).

6 Conclusion

A new and completely different algorithm and computer program, KODAC, was developed for precise satellite orbit determination using the ionospheric-free TD GPS carrier phase as the main observable. Unlike the traditional satellite orbit determination methods which rely on precise satellite dynamics models, this new method uses a purely kinematic approach. Since the GPS signals have enough spatial geometric information, it is possible to determine the satellite orbit in a purely kinematic mode. The algorithm assumes that the GPS satellite ephemerides, ground station

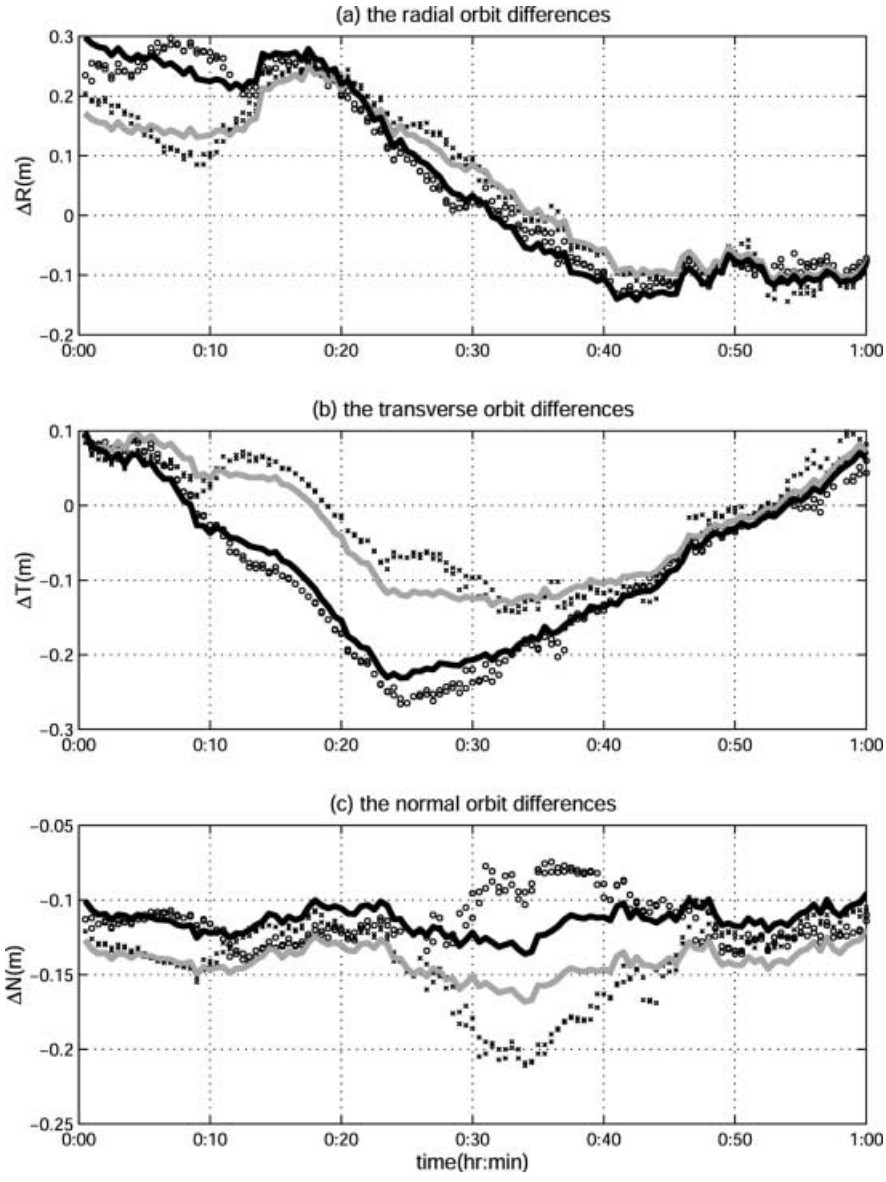

Fig. 10. Comparison of the sequential batch filter (circles and crosses) and the multi-epoch batch filter (*solid lines*) orbit solutions (sol0). *Dark color* denotes forward iteration and *light color* denotes backward iteration

positions, and the time series of the wet component of the tropospheric zenith delay are known in advance. The GPS carrier-phase data from the TOPEX/POSEIDON GPS receiver and the IGS ground stations were used for this study. A final RMS of the radial orbit differences of 8 cm was achieved when compared to the MSODP orbit, a solution based on dynamic orbit determination.

This new kinematic approach has the advantage of providing consistent orbit accuracy regardless of satellite altitude. The same data processing algorithm can be applied to any satellite with an on-board GPS receiver due to the algorithm's non-dynamic approach. When the satellite orbit accuracy requirement is not less than 10 cm in the radial direction, the combination of the sequential batch filter and the multi-epoch batch filter can be a sufficient tool for satellite orbit determination in the kinematic mode. The KODAC program can also be used as an alternative verification tool for other orbit determination programs due to its unique algorithm, which is quite different from the traditional dynamics-based approach.

Table 8. RMS of differences between the multi-epoch batch filter and the MSDOP orbit solutions: final iterations

Case	Direction	ΔR (m)	ΔT (m)	ΔN (m)	Total (m)
sol0	fwd	0.1294	0.0813	0.1415	0.2082
	bwd	0.1696	0.1257	0.1140	0.2400
sol1	fwd	0.1117	0.0756	0.1373	0.1925
	bwd	0.1544	0.1197	0.1102	0.2243
sol2	fwd	0.1151	0.0828	0.2549	0.2917
	bwd	0.0963	0.0436	0.2313	0.2543
sol3	fwd	0.0824	0.0829	0.2549	0.2804
	bwd	0.0480	0.0437	0.2313	0.2402

Acknowledgements. The work described in this paper was performed at the Center for Space Research, the University of Texas at Austin. The writing and publication of this paper was supported

by the Jet propulsion Laboratory, California Institute of Technology, under a contract with the National Aeronautics and Space Administration.

References

Bertiger W, Bar-Sever Y, Christensen E, Davis E, Guinn J, Haines B, Ibanez-Meier R, Jee J, Lichten S, Melbourne W, Mullerschoen R, Munson T, Vigue Y, Wu S, Yunck T (1994) GPS precise tracking of TOPEX/POSEIDON: results and implications. J Geophys Res 99(C12): 24 449–24 464

Brogen WL (1991) Modern control theory, 3rd edn. Prentice Hall, Englewood Cliffs, NJ

Byun SH (1998) Satellite orbit determination using GPS carrier phase in pure kinematic mode, PhD Thesis, Department of Aerospace Engineering and Engineering Mechanics, The University of Texas at Austin, Austin, TX

Byun SH, Schutz BE (2001) Improving satellite orbit solution using double-differenced GPS carrier phase in kinematic mode. J Geod 75: 533–543

Goad CC, Grejner-Brzezinska DA, Yang M (1996) Determination of high-precision GPS orbit using triple differencing technique. J Geod 70: 655–662

Hofmann-Wellenhoff B, Lichtenegger H, Collins J (2001) GPS: theory and practice, 5th edn. Springer, Berlin, Heidelberg, New York

Leick A (1995) GPS satellite surveying, 2nd edn. Wiley-Interscience, New York

Melbourne WG, Davis E, Yunck TP, Tapley B (1994) The GPS fight experiment on TOPEX/POSEIDON. Geophys Res Lett 21(19): 2171–2174

Press WH, Flannery BP, Teukolsky SA, Vetterling WT (1992) Numerical recipes in FORTRAN: the art of scientific computing, 2nd edn., Cambridge University Press, Cambridge

Remondi BW (1984) Using the global positioning system (GPS) phase observable for relative geodesy: modeling, processing and results. PhD Thesis, Department of Aerospace Engineering and Engineering Mechanics, The University of Texas at Austin, Austin, TX

Rim HJ (1992) TOPEX orbit determination using GPS tracking system. PhD Thesis, Department of Aerospace Engineering and Engineering Mechanics, The University of Texas at Austin, Austin, TX

Rim HJ, Webb CE, Byun SH, Schutz BE (2000) Comparison of GPS-based precision orbit determination approaches for IECSat. Spacefight Mechanics 2000, Clearwater, FL, pp 635–647

Solub GH, Van Loan CF (1996) Matrix computations, 3rd edn. The Johns Hopkins University Press, Baltimore, MD

Tapley B (1973) Statistical orbit determination Theory. In: Tapley B, Szebehely V (eds) Proceedings in recent advances in dynamical astronomy, pp 396–425. D. Reidel, Dordrecht